Article

Cell Reports

Somatic Mutations Activating the mTOR Pathway in Dorsal Telencephalic Progenitors Cause a Continuum of Cortical Dysplasias

Graphical Abstract

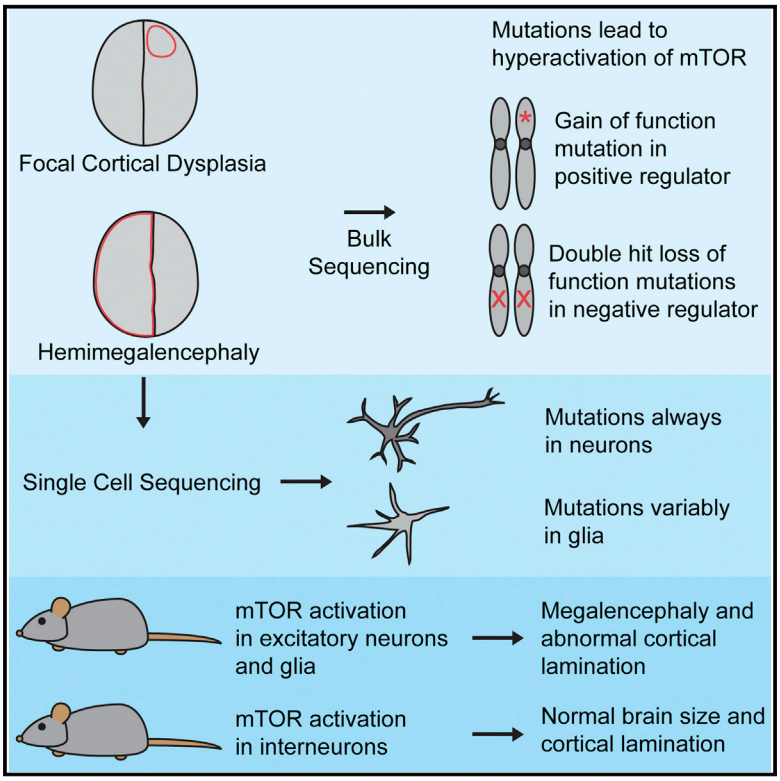

Highlights

- FCD and HME represent a disease continuum rather than discrete diseases
- Targeted deep sequencing of brain tissue identified an etiology in 41% of cases
- Two HME cases directly show a two-hit model of germline and somatic *TSC2* mutations
- mTOR activation in the excitatory neuron lineage is critical for dysplasia formation

Authors

Alissa M. D'Gama, Mollie B. Woodworth, Amer A. Hossain, ..., Ingmar Blümcke, Annapurna Poduri, Christopher A. Walsh

Correspondence

christopher.walsh@childrens.harvard.edu

In Brief

D'Gama et al. expand the genetic etiology of FCD and HME, including demonstration of a "two-hit" mutation model, and show that the diseases represent a spectrum caused by somatic mutations that activate the mTOR pathway in the dorsal telencephalic lineage.

D'Gama et al., 2017, Cell Reports *21*, 3754–3766
December 26, 2017
https://doi.org/10.1016/j.celrep.2017.11.106

CellPress

OPEN ACCESS
CellPress

Cell Reports
Article

Somatic Mutations Activating the mTOR Pathway in Dorsal Telencephalic Progenitors Cause a Continuum of Cortical Dysplasias

Alissa M. D'Gama,[1,2,3] Mollie B. Woodworth,[1,2,3] Amer A. Hossain,[1,2,3] Sara Bizzotto,[1,2,3] Nicole E. Hatem,[1,2,3] Christopher M. LaCoursiere,[4] Imad Najm,[5] Zhong Ying,[5] Edward Yang,[6,7] A. James Barkovich,[8] David J. Kwiatkowski,[9] Harry V. Vinters,[10] Joseph R. Madsen,[11] Gary W. Mathern,[12] Ingmar Blümcke,[5,13] Annapurna Poduri,[4,14] and Christopher A. Walsh[1,2,3,15,*]

[1]Division of Genetics and Genomics, Manton Center for Orphan Disease, and Howard Hughes Medical Institute, Boston Children's Hospital, Boston, MA 02115, USA
[2]Departments of Pediatrics and Neurology, Harvard Medical School, Boston, MA 02115, USA
[3]Broad Institute of MIT and Harvard, Cambridge, MA, 02142, USA
[4]Department of Neurology, Boston Children's Hospital, Harvard Medical School, Boston, MA 02115, USA
[5]Epilepsy Center, Cleveland Clinic, Cleveland, OH 44195, USA
[6]Department of Radiology, Boston Children's Hospital, Boston, MA 02115, USA
[7]Department of Radiology, Harvard Medical School, Boston, MA 02115, USA
[8]Departments of Radiology and Diagnostic Imaging, Neurology, Pediatrics, and Neurosurgery, University of California, San Francisco, San Francisco, CA 94143, USA
[9]Brigham and Women's Hospital, Harvard Medical School, Boston, MA 02115, USA
[10]Departments of Pathology and Laboratory Medicine (Neuropathology) and Neurology, David Geffen School of Medicine, University of California, Los Angeles, Los Angeles, CA, USA
[11]Department of Neurosurgery, Boston Children's Hospital, Boston, MA, USA
[12]Departments of Neurosurgery and Psychiatry and Biobehavioral Medicine, David Geffen School of Medicine, University of California, Los Angeles, Los Angeles, CA 90095, USA
[13]Department of Neuropathology, University Hospital Erlangen, Schwabachanlage 6, 91054 Erlangen, Germany
[14]Epilepsy Genetics Program, Division of Epilepsy and Clinical Neurophysiology, Department of Neurology, Boston Children's Hospital, Boston, MA 02115, USA
[15]Lead Contact
*Correspondence: christopher.walsh@childrens.harvard.edu
https://doi.org/10.1016/j.celrep.2017.11.106

SUMMARY

Focal cortical dysplasia (FCD) and hemimegalencephaly (HME) are epileptogenic neurodevelopmental malformations caused by mutations in mTOR pathway genes. Deep sequencing of these genes in FCD/HME brain tissue identified an etiology in 27 of 66 cases (41%). Radiographically indistinguishable lesions are caused by somatic activating mutations in *AKT3*, *MTOR*, and *PIK3CA* and germline loss-of-function mutations in *DEPDC5*, *NPRL2*, and *TSC1/2*, including *TSC2* mutations in isolated HME demonstrating a "two-hit" model. Mutations in the same gene cause a disease continuum from FCD to HME to bilateral brain overgrowth, reflecting the progenitor cell and developmental time when the mutation occurred. Single-cell sequencing demonstrated mTOR activation in neurons in all lesions. Conditional *Pik3ca* activation in the mouse cortex showed that mTOR activation in excitatory neurons and glia, but not interneurons, is sufficient for abnormal cortical overgrowth. These data suggest that mTOR activation in dorsal telencephalic progenitors, in some cases specifically the excitatory neuron lineage, causes cortical dysplasia.

INTRODUCTION

Focal malformations of cortical development (MCDs), including focal cortical dysplasia (FCD) and hemimegalencephaly (HME), are caused by somatic activation of the mammalian target of rapamycin (mTOR) pathway and represent the most important causes of surgically treated intractable childhood epilepsy (Blümcke et al., 2017; Harvey et al., 2008). FCDs, classified into several subtypes by the International League Against Epilepsy (Blümcke et al., 2011), involve small regions of radiographically and histopathologically abnormal cortex, whereas HME shows abnormal enlargement of much or all of a cerebral hemisphere (Blümcke et al., 2011; Poduri et al., 2012). Patients present with seizures that can be refractory to medical management (Kwan et al., 2010) and often require surgical resection of the abnormal brain tissue for seizure control (Aronica and Crino, 2014), allowing direct study of that tissue.

Although it has long been recognized that tuberous sclerosis complex (TSC), a multisystem disorder caused by loss-of-function mutations in *TSC1* or *TSC2*, is associated with abnormal activation of the mTOR pathway (Lipton and Sahin, 2014), recent

work has identified somatic activating mutations in *MTOR* itself, and genes encoding positive regulators of *MTOR*, in both FCD and HME (Jansen et al., 2015; Lee et al., 2012; Lim et al., 2015; Poduri et al., 2012). Several genes have also been described that act analogously to *TSC1* and *TSC2* as negative regulators of *MTOR*, causing FCD and HME via germline loss-of-function mutation coupled to demonstrated or inferred somatic loss of the second allele (Baulac et al., 2015; D'Gama et al., 2015; Lim et al., 2017; Scheffer et al., 2014; Sim et al., 2016; Weckhuysen et al., 2016). Surprisingly, TSC mutations can cause isolated FCD or HME in the absence of widespread hamartomas (D'Gama et al., 2015; Hoelz et al., 2017; Lim et al., 2017).

Several crucial questions remain about cortical dysplasia pathogenesis, including the cell type in which mTOR pathway activation leads to dysplasia and epilepsy and whether the distinct topographic distributions of FCD and HME correspond to somatic mutations in different neuronal or glial subtypes. For example, the focal distribution of FCD mirrors the relative clustering of excitatory neuronal clones (Gao et al., 2014), whereas the hemispheric dispersion of mutant cells in HME mirrors the clonal distribution of interneurons, suggesting that these two lesions might reflect mutations in excitatory or inhibitory neuronal lineages, respectively.

Here we identify causative mutations in *AKT1*, *AKT3*, *DEPDC5*, *MTOR*, *NPRL2*, *PIK3CA*, *PIK3R2*, *TSC1*, and *TSC2* in 18 FCD, HME, and polymicrogyria (PMG) cases, including isolated HME cases with "two-hit" germline and somatic *TSC2* mutations. Single-cell analyses of mutation-positive cases demonstrate that abnormal activation of the mTOR pathway in neurons is necessary and sufficient to cause epileptogenic MCDs. Mouse models show that abnormal activation of the mTOR pathway in the Emx-1-expressing lineage, which gives rise to excitatory neurons and some glia, is sufficient to cause abnormal cortical lamination and overgrowth, whereas such activation in inhibitory interneurons causes only subtle defects in cortical interneuron number. Overall, we show that FCD and HME are part of a spectrum of diseases caused by mutations that activate the mTOR pathway in dorsal telencephalic progenitors that give rise to excitatory neurons and, in some cases, glia.

RESULTS

Targeted Ultra-Deep Sequencing Identifies Mutations in Focal MCDs

We performed targeted ultra-deep sequencing on DNA extracted from surgically resected brain, blood, and/or buccal samples from 52 FCD, 38 HME, and 5 polymicrogyria cases (Figure S1). They included patients studied previously (D'Gama et al., 2015; Poduri et al., 2012) in whom no pathogenic variant was identified and new samples. DNA was sequenced using two custom panels targeting 12 mTOR pathway genes: *AKT1*, *AKT3*, *CCND2*, *DEPDC5*, *MTOR*, *PIK3CA*, *PIK3R2*, *PTEN*, *TSC1*, and *TSC2* in both panels and *NPRL2* and *NPRL3* only in panel 2, which achieved coverage >5,000×. We performed several analyses to identify high-quality, rare, and protein-altering variants and validated all variants using Sanger sequencing, digital droplet PCR (ddPCR), and/or subcloning (Experimental Procedures; Supplemental Experimental Procedures). Variants were considered pathogenic when they were loss-of-function variants, predicted deleterious missense variants proven pathogenic by functional studies, and/or variants previously identified in FCD, HME, or related syndromes. In total, we identified and validated 19 pathogenic variants in *AKT1*, *AKT3*, *DEPDC5*, *MTOR*, *NPRL2*, *PIK3CA*, *PIK3R2*, *TSC1*, and *TSC2* in 18 patients (Table 1; Figure 1; Tables S1, S2, S3, and S4).

Pathogenic Variants Identified in FCD

In four patients with FCD, we identified loss-of-function mutations in negative regulators of the mTOR pathway: *DEPDC5*, *NPRL2*, *TSC1*, and *TSC2*. Patient FCD-11, with a right frontotemporal FCD IIa, harbors *DEPDC5* variant p.R874*, previously identified in focal epilepsy (Lal et al., 2014). Patient FCD-13, with a left superior frontal gyrus FCD IIa, has *NPRL2* variant p.Q188*. Patient FCD-10, with a left frontal FCD, has the somatic nonsense *TSC2* variant p.R751*, previously identified in TSC (Jones et al., 1999) and detected in brain but not blood. We were unable to obtain additional medical records to ascertain whether this patient has additional TSC features. Patient FCD-12, with a left frontal FCD IIb (Figure 1G) and no other TSC features, harbors the somatic nonsense *TSC1* variant p.Q55*, previously identified in TSC (Leiden Open Variation Database [LOVD]). We did not identify germline mutations in *TSC1* or *TSC2* in either of these cases, further suggesting that both patients had isolated FCD and not syndromic TSC. Somatic TSC mutation without detectable germline mutation has recently been reported in FCD (Lim et al., 2017).

In an additional four patients with FCD, we identified somatic missense mutations in *MTOR* that were recently reported in FCD (Lim et al., 2015; Nakashima et al., 2015) and/or shown to activate mTOR (Grabiner et al., 2014): patient FCD-6, with a left frontoparietal FCD IIb (Figure 1B), has *MTOR* variant p.L1460P; patient FCD-7, with a left temporal FCD (Figure 1C), has *MTOR* variant p.S2215Y; patient FCD-8, with a left hemisphere FCD IIb, has *MTOR* variant p.C1483R; and patient FCD-14, with a left hemisphere FCD (Figure 1E), has *MTOR* variant p.T1977R detected in brain but not blood. Overall, the percentage of cells carrying the pathogenic mutations ranged from 2%–20.6% for the six patients with FCD and identified somatic mutations (Figure 1A).

Pathogenic Variants Identified in HME

In eight patients with HME, we identified mutations in *AKT1*, *AKT3*, *MTOR*, *PIK3CA*, and *TSC2*. Patient HME-19, with left HME and systemic physical findings consistent with Proteus syndrome, has the somatic *AKT1* variant p.E17K, previously identified in Proteus syndrome (Lindhurst et al., 2011). Patient HME-12, with left HME (Figure 1F), has the paralogous somatic *AKT3* variant p.E17K, detected in brain but not blood, which was initially identified in another HME patient by our lab (Poduri et al., 2012).

Three patients harbor somatic missense mutations in *MTOR* that were recently reported in FCD (Lim et al., 2015; Nakashima et al., 2015) but, to our knowledge, have not been reported in HME: patient HME-13, with right HME (Figure 1H), has *MTOR*

Table 1. Pathogenic Mutations and Likely Pathogenic Variant Detected in the mTOR Pathway in Patients with FCD, HME, and PMG with Megalencephaly

Subject	Diagnosis	Gene	Mutation	HGVS	Type	AAF	Comments
HME-19	HME, Proteus	*AKT1*	ms	p.E17K	somatic	8.1%–9.3% brain	previously identified in Proteus syndrome (Lindhurst et al., 2011)
HME-12	HME	*AKT3*	ms	p.E17K	somatic (not in blood)	3.4%–4.4% brain, 0% blood	previously identified in HME (Jansen et al., 2015; Lee et al., 2012; Poduri et al., 2012)
FCD-11	FCD IIa	*DEPDC5*	ns	p.R874*	germline	47.7% brain, 52.4% blood	loss of function, previously identified in focal epilepsy (Lal et al., 2014)
FCD-6	FCD IIb	*MTOR*	ms	p.L1460P	somatic	2.3%–2.6% brain	previously identified in FCD (Mirzaa et al., 2016; Møller et al., 2016; Nakashima et al., 2015); functional studies suggest pathogenic (Grabiner et al., 2014)
FCD-7	FCD	*MTOR*	ms	p.S2215Y	somatic	2.5%–2.8% brain	previously identified in FCD (Møller et al., 2016; Nakashima et al., 2015); functional studies suggest pathogenic (Grabiner et al., 2014)
FCD-14	FCD	*MTOR*	ms	p.T1977R	somatic (not in blood)	2.8%–4.7% brain, 0% blood	functional studies suggest pathogenic (Grabiner et al., 2014)
HME-13	HME	*MTOR*	ms	p.S2215Y	somatic	7.1%–8.3% brain	previously identified in FCD (Møller et al., 2016; Nakashima et al., 2015); functional studies suggest pathogenic (Grabiner et al., 2014)
HME-9	HME	*MTOR*	ms	p.T1977K	somatic (not in blood)	9.0%–10.4% brain, 0% blood	previously identified in FCD (Lim et al., 2015); functional studies suggest pathogenic (Grabiner et al., 2014)
FCD-8	FCD IIb	*MTOR*	ms	p.C1483R	somatic	10.0%–10.6% brain	previously identified in FCD (Lim et al., 2015); functional studies suggest pathogenic (Grabiner et al., 2014)
HME-14	HME	*MTOR*	ms	p.S2215F	somatic (not in blood)	18.3%–20.6% brain, 0% blood	previously identified in FCD (Lim et al., 2015; Mirzaa et al., 2016; Møller et al., 2016; Nakashima et al., 2015); functional studies suggest pathogenic (Grabiner et al., 2014)
PMG-1	PMG, macrocephaly	*MTOR*	ms	p.C1483Y	*de novo* germline	49.5% blood	previously identified in HME (Lee et al., 2012); functional studies suggest pathogenic (Grabiner et al., 2014)
FCD-13	FCD IIa	*NPRL2*	ns	p.Q188*	germline	31.7%–50.9% brain, 32.1%–51.1% blood	loss of function
HME-22	HME	*PIK3CA*	ms	p.E542K	somatic (not in blood)	15.9%–17.4% brain, 0% blood	previously identified in CLOVES (Kurek et al., 2012) and HME (D'Gama et al., 2015; Jansen et al., 2015)
PMG-2	PMG, macrocephaly	*PIK3R2*	ms	p.K376E	germline	50% blood	previously identified in BPP (Mirzaa et al., 2015)
FCD-12	FCD IIb	*TSC1*	ns	p.Q55*	somatic	5.1%–6.7% brain	previously identified in TSC (LOVD)
FCD-10	FCD	*TSC2*	ns	p.R751*	somatic (not in blood)	1.0% brain, 0% blood	loss of function, previously identified in TSC (Jones et al., 1999)
HME-11	HME	*TSC2*	fs	p.Y587*	somatic (not in blood)	3.1%–3.8% brain, 0% blood	loss of function, AA change previously identified in TSC (LOVD)
HME-15	HME	*TSC2*	ms	p.E1558K	somatic	7.5%–11.6% brain	previously identified in TSC (Dabora et al., 2001)
HME-15	HME	*TSC2*	ms	p.L631P	germline	47.4% brain	likely pathogenic, predicted deleterious

AAF, alternate allele frequency; BPP, bilateral perisylvian polymicrogyria; CLOVES, congenital lipomatous overgrowth, vascular malformations, epidermal nevis, spinal/skeletal anomalies/scoliosis; FCD, focal cortical dysplasia; Fs, frameshift; HGVS, Human Genome Variation Society; ms, missense; ns, nonsense; PMG, polymicrogyria; TSC, tuberous sclerosis complex. See also Figure S1 and Tables S1 and S2.

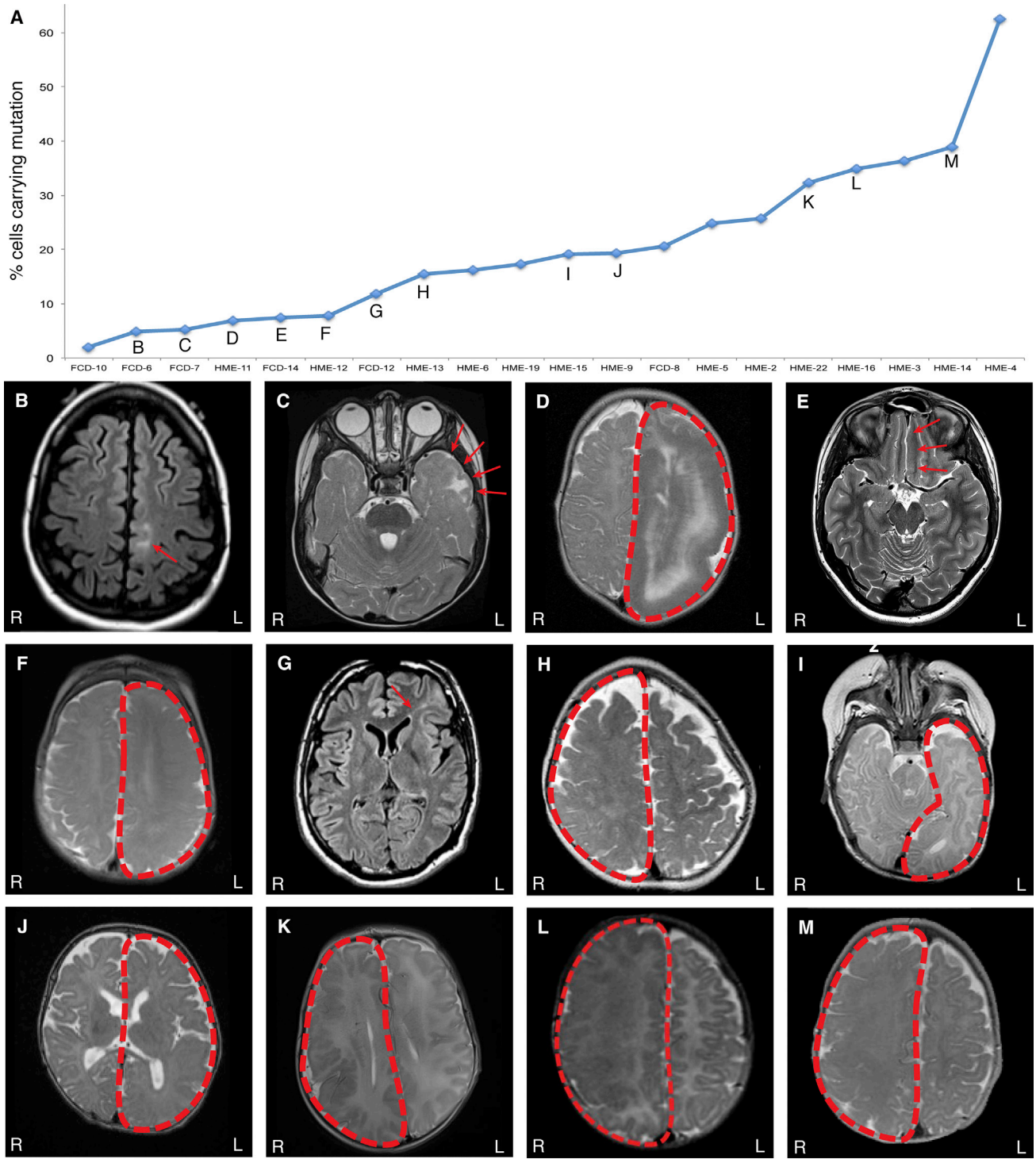

Figure 1. Somatic Mutations Leading to Abnormal Activation of the mTOR Pathway Are Identified Across a Spectrum of Somatic Cortical Dysplasias and a Continuum of AAFs

(A) Somatic mutations identified in FCD and HME cases in this study and our previous studies (D'Gama et al., 2015; Poduri et al., 2012) are graphed according to the percentage of cells carrying the somatic mutation.

(B–M) MRI of mutation-positive cases: FCD-6 (B), FCD-7 (C), HME-11 (D), FCD-14 (E), HME-12 (F), FCD-12 (G), HME-13 (H), HME-15 (I), HME-9 (J), HME-22 (K), HME-16 (L), and HME-14 (M). Although lesions with the lowest mosaicism are all FCD, and those with the highest are all HME, there is substantial overlap, suggesting that they form a continuum in terms of mosaicism. FCD, focal cortical dysplasia; HME, hemimegalencephaly.

Patient identifying information, words, numbers, and bars have been removed.

variant p.S2215Y; patient HME-9, with left HME (Figure 1J), has *MTOR* variant p.T1977K, detected in brain but not blood; and patient HME-14, with right HME (Figure 1M), has *MTOR* variant p.S2215F, also detected in brain but not blood. In addition, patient HME-22, with right HME (Figure 1K), has the somatic *PIK3CA* variant p.E542K, detected in brain but not blood, which was initially identified in HME in another HME patient by our lab (D'Gama et al., 2015).

Two-Hit TSC2 Variants Identified in Isolated HME

In two patients with isolated HME, we detected two-hit germline plus somatic mutations in *TSC2.* Patient HME-15, who presented with infantile spasms and left HME (Figure 1I), has a predicted deleterious germline missense variant in *TSC2*, p.L631P, and a somatic missense variant in *TSC2*, p.E1558K, which was previously identified in TSC (Dabora et al., 2001). Patient HME-11, who presented with hypomotor, tonic, and clonic seizures and left HME (Figure 1D), has a germline missense variant in *TSC2*, p.R1713H, which we identified in our previous study (D'Gama et al., 2015) and which was also previously identified in TSC (Hirfanoglu and Gupta, 2010; Hoogeveen-Westerveld et al., 2011), as well as a somatic frameshift variant in *TSC2*, p.Y587*, detected in brain but not blood; the same mutation has been previously identified in TSC (LOVD). Although we acknowledge the age dependence of syndromic TSC manifestations, based on available records and specialized pediatric neurology examinations, both patients lacked any signs of syndromic TSC, and brain MRIs did not show other TSC hallmarks. These findings are remarkable because TSC mutations have not previously been associated with isolated HME and because capturing both germline and somatic mutations in TSC-associated cortical dysplasia is uncommon (Lim et al., 2017). The percentage of cells carrying the pathogenic mutations ranged from 6.2%–41.2% for the eight patients with HME and identified somatic mutations (Figure 1A).

Overall Yield

Our current and previous studies (D'Gama et al., 2015; Poduri et al., 2012) have identified pathogenic mutations in 41% (27 of 66) of the focal MCD cases for whom brain tissue was available (10 of 38 FCD, 26%; 17 of 28 HME, 61%) and none (0 of 33) of the cases for whom brain tissue was not available (Figure 2; Table S4). In all cases for which both brain and non-brain samples were available (2 FCD and 7 HME cases), pathogenic somatic mutations were identified only in brain. This suggests that most pathogenic mutations in FCD and HME arise relatively late during embryonic development and are likely "brain-only," and that testing of blood DNA is generally not useful diagnostically.

Pathogenic Variants Identified in PMG with Megalencephaly

We identified a *de novo* germline missense variant in *MTOR*, p.C1483Y, in patient PMG-1, with bilateral perisylvian PMG, megalencephaly, multiple congenital anomalies, and death at the age of 2 years because of respiratory failure; this variant was previously reported in the somatic state in an HME case (Lee et al., 2012). A germline mutation of the same amino acid, p.C1483F, has previously been reported in a patient with megalencephaly and intractable epilepsy who died at 19 months because of respiratory failure (Kingsmore et al., 2013). We also identified a germline missense variant in *PIK3R2*, p.K376E, in patient PMG-2, with bilateral perisylvian PMG with megalencephaly; this variant was recently identified in a case with bilateral perisylvian PMG (Mirzaa et al., 2015).

Pathogenic Somatic Mutations Are Present in the Neuronal Lineage

To define the minimal cell types in cortical dysplasias, we sorted single nuclei from seven genetically characterized cases using an antibody against NeuN, performed whole-genome amplification using multiple displacement amplification, and genotyped the mutations as described previously (Evrony et al., 2012; Experimental Procedures; Figure 3; Table S5). In two FCD and two HME cases, the identified somatic mutations were strongly enriched in neuronal compared with non-neuronal cells, including both cases with the smallest lesion and smallest proportion of cells carrying the mutation. Patient FCD-6 carries *MTOR* variant p.L1460P in 4.6%–5.2% of cells based on next-generation sequencing (NGS), with 7.1% ± 1.8% of NeuN+ cells and 0.53% ± 0.53% of NeuN− cells carrying the mutation ($p < 0.001$, two-tailed Fisher's exact test). Patient FCD-14 carries *MTOR* variant p.T1977R in 5.6%–9.4% of cells based on NGS, with 24% ± 4.2% of NeuN+ cells and 0% of NeuN− cells carrying the mutation ($p < 0.0001$). Patient HME-16 (HMG-3 from Poduri et al., 2012) carries *AKT3* mutation p.E17K in ≈35% of cells based on subcloning, with 60% ± 5.2% of NeuN+ cells and 26.8% ± 4.9% of NeuN− cells carrying the mutation ($p < 0.0001$). Patient HME 23 carries *PIK3CA* variant p.E545K (independently identified) in 47% of cells based on ddPCR, with 77% ± 4.5% of NeuN+ cells and 24.4% ± 6.4% of NeuN− cells carrying the mutation ($p < 0.00000001$). These results suggest that somatic mutations involving the smallest numbers of cells are strongly enriched in neuronal compared with glial cells during development. Larger FCD lesions showed mutations in neuronal and non-neuronal cells ($p > 0.05$), and one HME case showed modest enrichment in NeuN− compared with NeuN+ cells ($p < 0.0001$). These data suggest that somatic mutations associated with FCD and HME can occur in progenitors that generate both neuronal and non-neuronal cells, but in some cases occur in neuron-specific progenitors. In all cases, the mutation is present in >5% of neuronal cells, suggesting that activation of the mTOR pathway in the neuronal lineage is obligatory for the abnormal cortical development underlying FCD and HME. However, these data do not identify whether mTOR activity in excitatory or inhibitory neurons is essential for dysplasia formation.

mTOR Pathway Activation in Dorsal Telencephalic Progenitors Is Sufficient to Cause Abnormal Cortical Lamination and Overgrowth

We explored the importance of abnormal mTOR activation in excitatory versus inhibitory cortical neurons using mouse models with cell-type-specific mTOR pathway activation via conditional expression of constitutively active *Pik3ca* p.H1047R, a mutation associated with both FCD and HME (D'Gama et al., 2015; Jansen et al., 2015), in either the dorsal telencephalic lineage (*Emx1-Cre;Pik3ca* $^{H1047R/wt}$, referred to

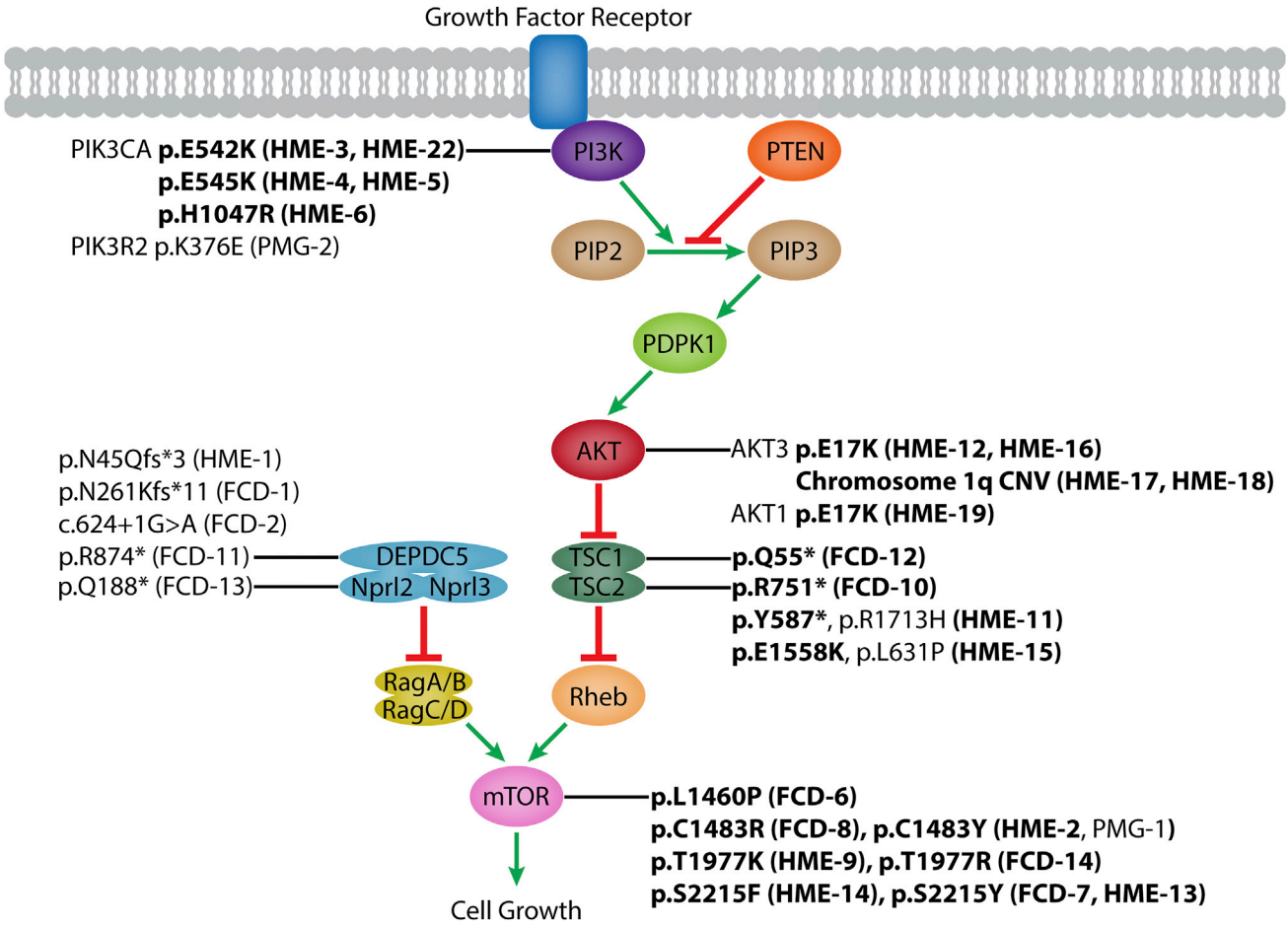

Figure 2. The mTOR Pathway and Identified Pathogenic Mutations

Schematic of the mammalian target of rapamycin (mTOR) pathway, annotated with pathogenic mutations identified by our lab (this study and our previous studies; D'Gama et al., 2015; Poduri et al., 2012). Somatic mutations are shown in boldface. FCD, focal cortical dysplasia; HME, hemimegalencephaly; PMG, polymicrogyria. See also Tables S3 and S4.

as "*Emx1-Cre*," which uses an Emx1-Cre and expresses in excitatory neurons and some glia) (Gorski et al., 2002) or in the interneuron lineage (*Nkx2.1-Cre;(ROSA)26-tdTomato* ^{fl}*/Pik3ca_H1047R*^{fl} mice, referred to as "*Nkx2.1-Cre*," which uses an Nkx2.1-Cre and also expresses tdTomato in the interneuron lineage). Conditional mTOR pathway activation in the Emx-1 expressing lineage leads to dramatic megalencephaly (Figures 4A–4M). The *Emx1-Cre* P7 cortex is significantly larger than the wild-type P7 cortex, with markedly abnormal gyrification in the cingulate cortex, neocortex, piriform cortex, and dentate gyrus (Figures 4A–4D and 4M), confirming recent results that abnormal activation of the mTOR pathway in excitatory neurons and glia causes cortical enlargement (Roy et al., 2015).

Markers of deep cortical layers, such as CTIP2, are expressed in the *Emx1-Cre* cortex at comparable levels and in generally similar numbers of cells as in the wild-type cortex (Figures 4E and 4F). Most CTIP2-positive deep-layer neurons in the *Emx1-Cre* cortex have migrated to an appropriate laminar position in layers V and VI, although some heterotopic cells expressing deep-layer markers breach the deep layers and reach the pial surface (arrow, Figure 4F). In contrast, superficial-layer gene expression and migration are significantly abnormal in the *Emx1-Cre* cortex (Figures 4G–4J). More neurons in the *Emx1-Cre* cortex express markers of superficial-layer neurons, such as CUX1 and SATB2, compared with the wild-type cortex. In addition, the laminar structure is markedly abnormal in superficial layers, with significant heterotopias and loss of normal sublaminar structure. Our results suggest that the generation and migration of excitatory cortical neurons are profoundly disrupted in the *Emx1-Cre* cortex.

Although mTOR activation in the dorsal telencephalic lineage creates dramatic megalencephaly, similar activation in the interneuron lineage does not cause detectable dysplasia, megalencephaly, or overgrowth (Figures 4N–4EE). We found no significant difference in total length of the neocortical surface between *Nkx2.1-Cre* and wild-type P7 mice (Figure 4N), consistent with the grossly normal brain seen in conditional knockout mice with *Tsc1* depletion in *Dlx5/6*-positive interneuron precursors (Fu et al., 2012). The genotypically wild-type excitatory neurons show normal cortical lamination and layer thickness

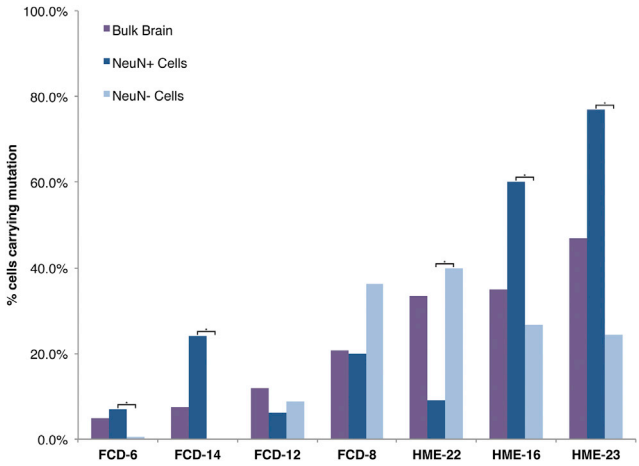

Figure 3. Pathogenic Somatic Mutations in FCD and HME Are Always Present in the Neuronal Lineage

Single neuronal and non-neuronal nuclei from patients FCD-6, FCD-8, FCD-12, FCD-14, HME-16, HME-22, and HME-23 were isolated using an antibody against NeuN. DNA was amplified, and genotyping was performed for the respective pathogenic mutations. The sequencing traces were analyzed to calculate the number of cells with the mutation, taking into account allelic dropout, as described previously (Evrony et al., 2012). The p values were calculated from cell counts using a two-tailed Fisher's exact test; asterisks indicate a significant difference in the percentage of cells carrying the mutation between the NeuN+ and NeuN− cell populations for that case. FCD, focal cortical dysplasia; HME, hemimegalencephaly. See also Table S5.

in the *Nkx2.1-Cre* brain, with both CTIP2- and SATB2-positive neurons migrating to appropriate positions, and no visible heterotopic cells (Figures 4O–4V). In contrast, the cortical interneuron number is abnormal in the *Nkx2.1-Cre* P7 brain, with significantly fewer interneurons compared with the wild-type brain (Figures 4W–4AA). These results show that expression of mutant PIK3CA in the interneuron lineage does not reproduce the severe phenotype found in the *Emx1-Cre* mutant. Overall, the mouse models show that abnormal activation of the mTOR pathway in the dorsal telencephalic, but not the interneuron, lineage is sufficient to cause abnormal cortical lamination and overgrowth. Taken together with our single-cell results demonstrating that pathogenic somatic mutations occur in neuron-specific progenitors in some cases, these data further suggest that abnormal activation of the mTOR pathway in the excitatory neuron lineage may be sufficient to cause focal MCDs in some cases.

DISCUSSION

In this study, we further elucidate the genetic etiology of FCD and HME and investigate the cell type specificity of abnormal mTOR activation in dysplasia pathogenesis. Our data confirm the association of mutations in *AKT1*, *AKT3*, *DEPDC5*, *MTOR*, *NPRL2*, *PIK3CA*, *TSC1*, and *TSC2* with FCD or HME and show that two-hit germline and somatic *TSC2* mutations can cause isolated HME. Single-cell analyses show that abnormal activation of the mTOR pathway is always present in the neuronal lineage but variably present in glia. Mouse model analyses show that mTOR pathway activation in the dorsal telencephalic lineage, but not the interneuron lineage, is sufficient to model cortical dysplasia. Overall, our results suggest that FCD and HME are not discrete diseases but rather represent a disease continuum caused by somatic mutations occurring throughout neurogenesis in progenitor cells that give rise to excitatory neurons and, in some cases, glia.

Our study highlights the relationship between depth of coverage in next-generation sequencing experiments and sensitivity to detect pathogenic somatic mutations. In our previous study, we identified a germline *TSC2* mutation in HME-11, and, in this study, the higher depth of coverage achieved allowed us to identify a previously undetectable second somatic *TSC2* mutation present in ≈7% of brain cells. We were only able to identify somatic mutations when brain tissue was available, and such mutations were present in as few as 2% of brain cells. The lack of mutation outside of the brain emphasizes that sequencing of brain tissue-derived DNA is required for genetic diagnosis in virtually all FCD and HME cases. The dependence of sensitivity on depth of coverage suggests that still more "unsolved" FCD cases may reflect somatic mutations present at even lower allele frequencies.

We implicate *TSC2* mutations in HME, supporting the application of Knudson's two-hit model of tumor pathogenesis (Knudson, 1971) to MCDs. This mechanism is well supported for non-nervous system tumors associated with TSC, such as renal cell carcinoma, but has only rarely been demonstrated for cerebral lesions (Crino et al., 2010; Qin et al., 2010; Tyburczy et al., 2015b). Similarly, a second hit has only once been identified in an FCD patient who carried germline and somatic mutations in *DEPDC5* (Baulac et al., 2015). Curiously, a recent report of somatic mutations in *TSC1* and *TSC2* in FCD cases failed to identify associated germline mutations (Lim et al., 2017), which would seem, in principle, easier to detect. We demonstrate germline and somatic mutations in *TSC2* from non-TSC patients and associated with HME. Our remaining cases with germline loss-of-function mutations may also contain "second-hit" mutations that could represent large-scale copy number variants (CNVs) undetectable by targeted sequencing, mutations in genes not included in our panel or in introns (Tyburczy et al., 2015a) or mutations below our detection limit.

Our single-cell analyses of mutation-positive cases show that the mutations are always present in the neuronal lineage and, in some cases, present in neuron-specific progenitors, suggesting that abnormal activation of the mTOR pathway in neurons is necessary and sufficient for the development of focal epileptogenic MCDs. Our *Emx1-Cre* mouse model demonstrates abnormal cortical overgrowth and cortical lamination defects. Although previous work has described the effect of *Pik3ca* p.H1047R expression beginning at late embryonic or neonatal ages (Roy et al., 2015), we generate mice with *Pik3ca* p.H1047R expression beginning at early embryonic age and examine cortical lamination and subtype identity postnatally, when this identity is typically fully acquired in the wild-type brain. Although Emx1-Cre is expressed in progenitors that produce all cortical excitatory neurons, expression of constitutively active *Pik3ca* p.H1047R specifically causes over-production of superficial-layer neurons, which are generated after deep-layer

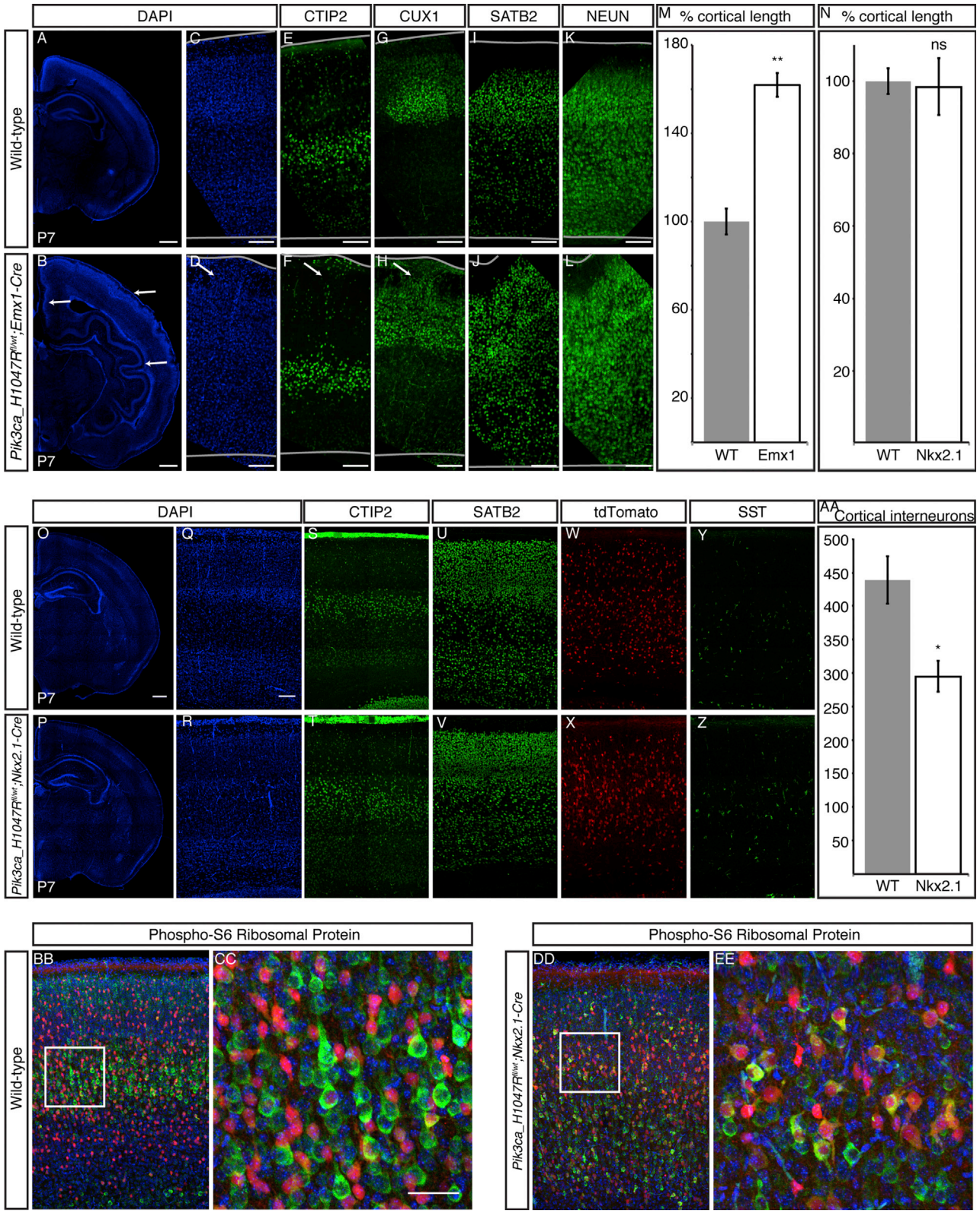

(legend on next page)

neurons. This has significant implications for human cortical dysplasia because the human cortex contains a relatively greater share of superficial-layer neurons, which are uniquely vulnerable to constitutively active *PIK3CA* expression, compared with the mouse cortex.

On the other hand, in our *Nkx2.1-Cre* mouse model, we do not see cortical overgrowth or cortical lamination defects and only find a subtle defect in cortical interneuron number. Previous mouse models have shown that conditional activation of mTOR in either neuronal or glial subsets can lead to abnormal cortical enlargement and seizures, generally using inactivation of *Tsc1*, *Tsc2*, or *Pten*; however, only mouse models with conditional activation of mTOR in neuron-containing lineages have shown cortical lamination defects (Magri et al., 2013; Meikle et al., 2007; Roy et al., 2015; Uhlmann et al., 2002; Zeng et al., 2011; Zhou et al., 2009). Thus, our data suggest that the cortical lamination defects seen in cortical dysplasia may be due to mutant excitatory neurons. However, mutant glia and neuron-glia interactions may also be contributing to cortical dysplasia pathogenesis, especially to abnormal cortical overgrowth and seizures, in cases where the somatic mutation occurs in a progenitor giving rise to both cell types. Together, our single-cell and mouse model analyses suggest that somatic mutations activating the mTOR pathway in dorsal telencephalic progenitors cause a continuum of cortical dysplasias, that activation in the excitatory neuron lineage is essential for dysplasia formation, and that activation in the excitatory neuron lineage is sufficient for dysplasia formation in some cases.

Given that somatic mutations are frequent, it is reasonable to assume that somatic mutations that activate the mTOR pathway sometimes occur in progenitor cells of the ganglionic eminences that give rise only to interneurons, but such a condition has yet to be described. The relatively normal appearance of the cerebral cortex in *Nkx2.1-Cre* mice suggests that such a mutation may not lead to a radiographically or histologically abnormal brain, as with FCD or HME, but may nonetheless disrupt the neuronal circuitry and contribute to the development of seizures (Fu et al., 2012), especially given the demonstrated decrease in cortical interneuron number. Families with germline mutations in *DEPDC5* have epilepsy, but only a few have radiographically detectable dysplasia (Scheffer et al., 2014). One possibility is that a somatic second-hit *DEPDC5* mutation in the inhibitory lineage may contribute to epilepsy in such patients without obvious dysplasia.

The widespread nature of HME initially suggested that it might reflect mutations in the clonally widespread interneuron lineage, whereas the focal nature of FCD suggested a defect of the excitatory lineage. In contrast, our data suggest that both lesions likely reflect mutations in dorsal telencephalic progenitors that normally give rise to excitatory neurons. Both the degree of mosaicism (Figure 1) and the radiographic extent of these two lesions appear to represent a continuum rather than separable distributions, further suggesting their related origin. In this scenario, the differing extent of smaller and larger lesions would instead reflect the time and place of origin of the somatic mutation in the dorsal cortical progenitor zone (Figure 5), as recently hypothesized (Blümcke and Sarnat, 2016; Cepeda et al., 2006). Our data and previous study have suggested that somatic mutations present at lower alternate allele frequencies (AAFs) in the human brain—that is, mutations present in a smaller number of cells—appear to arise later in development than mutations present at higher AAFs—that is, mutations present in a larger number of cells (Lodato et al., 2015).

Analyzing our results in combination with recent studies strongly supports a relationship between the allele frequency of a mutation and the resulting phenotype (Figure 6). For example, for patients carrying the p.S2215Y/F mutation in *MTOR*, fourteen patients with FCD, mostly FCD IIb, carry the mutation in 2.1%–18.6% of cells, and two patients with HME carry the mutation in 14.2%–41.2% of cells (Lim et al., 2015; Mirzaa et al., 2016; Møller et al., 2016; Nakashima et al., 2015). In fact, analyzing all of the somatic mutations reported in the literature associated with FCD and HME reveals that the average AAF for somatic mutations associated with FCD, 3.76% ± 2.89%, is significantly lower than the average AAF for somatic mutations associated with HME, 16.35% ± 9.26% ($p < 0.0001$, two-tailed t test) (Table S6). Thus, a larger fraction of cells carrying a

Figure 4. Conditional Expression of the Activating *Pik3ca* Mutation H1047R in Dorsal Telencephalic Progenitor Cells Causes Cortical Enlargement, Especially in Superficial Layers

(A–D) Compared with the wild-type P7 cortex (A and C), the *Emx1-Cre;Pik3ca*$^{H1047R/wt}$ P7 cortex (B and D) is larger, with marked gyrification in the cingulate cortex, neocortex, and piriform cortex (arrows in B and D).

(E–L) Deep-layer gene expression (CTIP2) is normal (E and F), with some heterotopic cells reaching the pial surface (arrow in F). Superficial-layer gene expression is increased in *Emx1-Cre* P7 cortex compared to wild-type P7 cortex, as shown by CUX1 (G and H) and SATB2 (I and J) staining, with significant heterotopias (arrow in H).

(M) The total length of the neocortical surface is significantly increased in *Emx1-Cre* mice compared with the wild-type.

(N) There is no significant difference in total length of the neocortical surface in *Nkx2.1-Cre;(ROSA)26-tdTomato* ^{fl}*/Pik3ca_H1047R*^{fl} P7 cortex compared with the wild-type.

(O–V) Compared with the wild-type P7 cortex (O and Q), there is no gyrification in *Nkx2.1-Cre* P7 cortex (P and R). Cortical lamination in the mutant is comparable with the wild-type, as shown by staining with markers of layers V and VI (CTIP2; S and T) and layers II/III and IV (SATB2; U and V).

(W–Z) Interneuron distribution in the mutant cortex layers is comparable with the wild-type, as shown by tdTomato-positive cells (W and X) and Somatostatin (SST) staining (Y and Z).

(AA) Interneuron number (tdTomato-positive cells) is significantly reduced in the *Nkx2.1-Cre* P7 cortex compared with the wild-type.

(BB–EE) Compared with the wild-type (BB and CC), most tdTomato-positive recombinant interneurons (red) in the *Nkx2.1-Cre* P7 cortex (DD and EE) are also positive for phospho-S6 ribosomal protein (green), an indicator of mTOR pathway activation.

n = 3. Unpaired t test. *$p < 0.05$, **$p < 0.01$. Data are represented as mean ± SEM. Scale bars, 500 μm (whole hemispheres) and 100 μm (cortex higher magnifications).

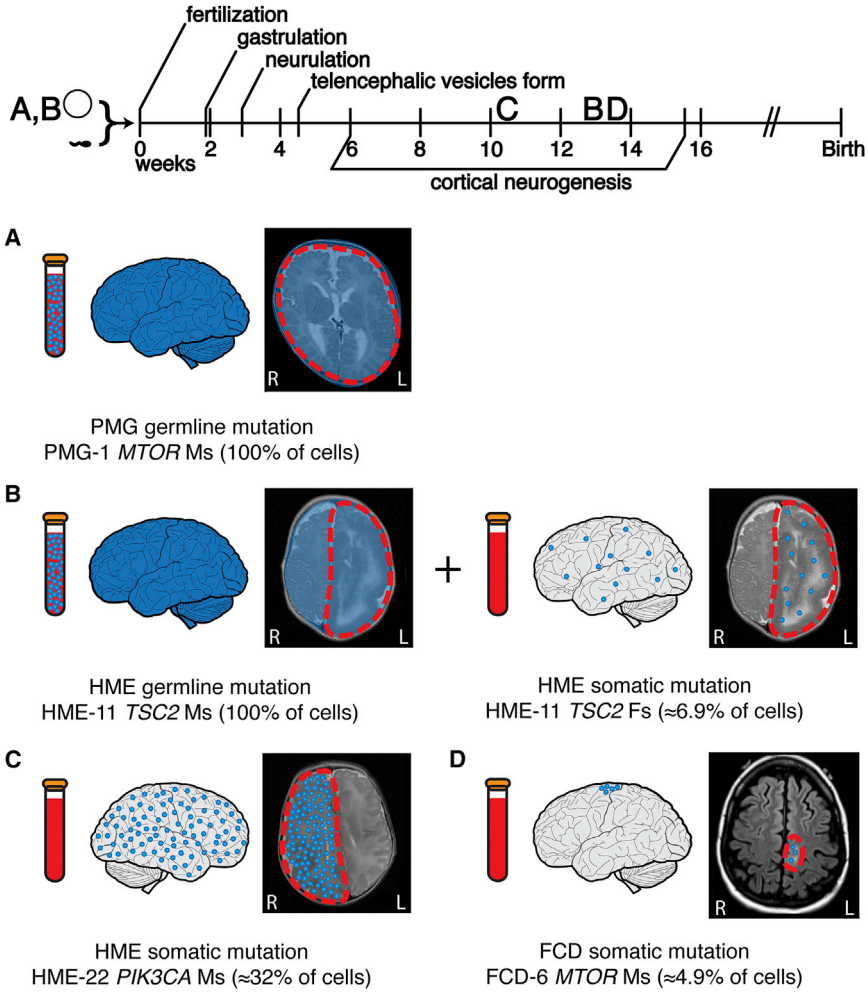

Figure 5. FCD and HME Represent a Continuum, with Lesion Differences Reflecting the Time and Place of Origin of the Mutation

(A) Germline mutations occur before fertilization and are detectable in the brain and a clinically accessible blood sample. Germline activating mutations in the mTOR pathway can lead to megalencephaly, as seen in case PMG-1 with a *de novo* germline *MTOR* mutation.

(B) Two-hit germline and somatic mutations in negative regulators of the mTOR pathway can lead to focal MCDs. In some cases, such as HME-11 with two *TSC2* mutations, we have identified both a germline and a somatic mutation leading to HME. The germline mutation was detectable in brain and blood, whereas the somatic mutation occurred later during embryonic development and was detectable only in brain.

(C) Activating somatic mutations in positive regulators of the mTOR pathway can also lead to focal MCDs. Mutations present at a higher AAF, suggesting that they arose earlier during cortical neurogenesis, appear more likely to lead to HME; for example, we identify a somatic activating point mutation in *PIK3CA* present in ≈32% of cells in the abnormal hemisphere of case HME-22.

(D) Mutations present at a lower AAF, suggesting that they arose later during cortical neurogenesis, appear more likely to lead to FCD; for example, we identify a somatic activating point mutation in *MTOR* present in ≈4.9% of the cells in the abnormal cortical tissue of case FCD-6. AAF, alternate allele frequency; FCD, focal cortical dysplasia; HME, hemimegalencephaly; PMG, polymicrogyria.

mutation, which suggests that the mutation arose earlier in development, appears to correlate with a "larger" MCD and a more severe phenotype. The two FCD cases in whom the pathogenic mutations were limited to neurons also showed the lowest AAFs, consistent with the suggestion that these limited mutations arose later during development, potentially after segregation of neuronal and glial lineages, compared with mutations present more broadly.

Comparison of our results with recent studies of functionally silent clonal somatic mutation in normal human brain (Lodato et al., 2015) suggests that mTOR gain-of-function produces a proliferative advantage, resulting in an approximately 10-fold enrichment of mutant cells compared with normal cells. Functionally silent somatic mutations that occupy focal shapes and volumes similar to FCD or hemispheric patterns similar to HME are present at much smaller alternative allele fractions than mTOR pathway mutations: 0.1%–1% versus 1%–10% for FCD-sized lesions; 1%–5% versus 5%–30% for HME-sized lesions (Evrony et al., 2015; Lodato et al., 2015). Mutations not affecting proliferation are also usually detected both in brain and non-brain tissues at AAFs $> \approx 5\%$ (Jamuar et al., 2014; Lodato et al., 2015), but mTOR mutations are limited to the brain, further supporting a proliferative advantage in the brain for mTOR mutations. This suggests that most FCD and HME mutations arise in dorsal cerebral cortical progenitors after the neural plate stage but show a relative growth advantage, allowing them to achieve higher clonal fractions than cells carrying functionally silent mutations.

Currently, patients with FCD and HME and intractable epilepsy rely on surgical resection for attempted seizure control. With our identification of mutations in *TSC1/2* in patients with FCD and HME, we provide further evidence linking FCD, HME, and TSC with the hope that mTOR inhibitors currently being studied in patients with TSC may be effective for patients with FCD and HME (Poduri, 2014). Recently, several mouse models of focal MCDs have shown alleviation of seizures upon treatment with mTOR pathway inhibitors (Baek et al., 2015; Lim et al., 2015; Roy et al., 2015). Clinical testing for somatic mutations is limited and currently requires submission of multiple tissue types, but our data suggest that analysis of brain tissue alone with deep sequencing strategies is sufficient to detect the relevant mutations. If emerging clinical trials require a tissue diagnosis, as is the case in the molecular treatment of somatic cancers (Xue and Wilcox, 2016), then clinical studies may need to adopt deep sequencing strategies of brain tissue from FCD and HME cases.

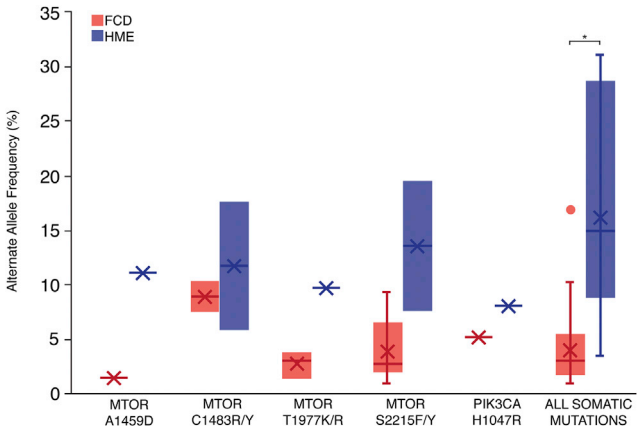

Figure 6. The Relationship between AAF and Disease Phenotype Is Evident for Both Individual Mutant Alleles and Overall Identified Mutations

After performing a literature review to identify all reported mutations associated with FCD and HME and their average AAFs, we identified individual mutant alleles associated with both FCD and HME. Because of the small number of cases associated with each mutant allele, p values were not calculated for individual alleles. Overall, the average AAF for somatic mutations associated with FCD is significantly lower than the average AAF for somatic mutations associated with HME ($p < 0.0001$, two-tailed t test). See also Table S6.

EXPERIMENTAL PROCEDURES

Patient Cohort

This study was approved by the institutional review boards of Boston Children's Hospital, University of California, Los Angeles, and the Cleveland Clinic. Subjects were identified and evaluated in a clinical setting, and biological samples were collected for research after obtaining written informed consent. 95 patients were included; 52 had FCD, 38 had HME, and 5 had PMG (4 of 5 with megalencephaly) based on MRI and neuropathology. Clinical information, including gender, for cases with identified variants is reported in Table S2.

DNA Sequencing and Analysis

Genomic DNA was extracted from patient samples using standard methods. We prepared libraries using two custom Haloplex panels (Agilent) according to the manufacturer's protocol and performed sequencing on HiSeq sequencers (Illumina). Further details regarding panel design, DNA library preparation, sequencing, and analysis are available in the Supplemental Experimental Procedures.

Validation of mTOR Pathway Variants

Rare and protein-altering (missense, nonsense, splice site, frameshift, and insertion-deletion) variants in the target genes were validated using Sanger sequencing. For potential somatic variants, validation was performed using ddPCR or subcloning. In addition, for potential somatic variants, ddPCR was performed on any additional samples that were not sequenced, and for all variants, segregation analysis was performed when parental DNA was available. Further validation details are available in the Supplemental Experimental Procedures.

Single-Nucleus Analysis

Isolation of single nuclei using fluorescence-activated nuclear sorting (FANS) with antisera to NeuN (Millipore, MAB377X) and whole-genome amplification using multiple displacement amplification (MDA) were performed as described previously (Evrony et al., 2012). Single nuclei from FCD-6, FCD-8, FCD-12, FCD-14, HME-16, HME-22, and HME-23 were isolated, amplified, and sequenced for their respective pathogenic mutations using PCR (GoTaq Hot Start DNA Polymerase, Promega). Analysis to calculate the number of cells with the mutation, taking into account allelic dropout, was performed as described previously (Evrony et al., 2012). For HME-16, we combined our current with our previous analysis (Evrony et al., 2012). Cell counts of NeuN+ and NeuN− populations with pathogenic mutations identified using single-nucleus analysis were compared using a two-tailed Fisher's exact test and corrected for multiple testing.

Mouse Models and Immunohistochemistry

All mouse studies were approved by the Boston Children's Hospital Institutional Animal Care and Use Committee (IACUC) and were performed in accordance with institutional and federal guidelines. *Emx1-Cre* (RRID, MGI_4440744; stock number 005628), *Nkx2.1-Cre* (RRID, MGI 3773076; stock number 008661), *Rosa26R-tdTomato-Ai9* (RRID, MGI_3809523; stock number 007909), and *Rosa26-Pik3ca_H1047R* (RRID, MGI_5000472; stock number 016977) mice were purchased from The Jackson Laboratory. Mice were housed with a standard 12-hr light/dark schedule (lights on at 07:00 a.m.), and mixed genders were used for all experiments.

Littermate pairs of experimental and control mice were collected on postnatal day 7 and transcardially perfused with 4% paraformaldehyde, and brains were dissected and post-fixed at 4°C overnight. Tissue was sectioned at 50-μm coronal sections on a vibrating microtome (Leica). Anatomically matched sections were selected from each mouse, and the somatosensory cortex was imaged by fluorescent microscopy (for montages) and confocal microscopy (for individual immunostains). Non-specific epitopes were blocked through 1 hr incubation at room temperature (RT) in 8% goat serum/0.3% bovine serum albumin or 10% normal donkey serum in PBS 1×) prior to incubation with primary antibody diluted in blocking solution at 4°C overnight. Secondary antibody incubation was performed for 1.5 hr at RT. For DAPI staining, tissue was either mounted in DAPI-Fluoromount-G (Southern Biotech) or incubated for 10 min with Hoechst 33342 (Thermo Fisher Scientific) diluted 1:5,000 in PBS 1× prior to mounting in Fluoromount G without DAPI (Southern Biotech). Primary antibodies were as follows: rabbit anti-Satb2 (1:300, Abcam, ab92446), rabbit anti-Ctip2 (1:300, Abcam, ab28448), rabbit anti-CDP1 (1:200, Santa Cruz Biotechnology, M-222), rabbit anti-phospho-S6 ribosomal protein (Ser235/236, 1:400, Cell Signaling Technology, 4858), mouse anti-NeuN (Millipore, MAB377), and rat anti-Somatostatin (1:50, Abcam, ab30788). Secondary antibodies were as follows: donkey anti-rabbit, donkey anti-rat, and goat anti-mouse Alexa Fluor 488 (1:800, Thermo Fisher Scientific). Fluorescently stained sections were imaged with a Zeiss LSM 700 confocal microscope driven by ZEN imaging software and equipped with a 10× Plan-Apochromat/NA 0.45 and a 20× Plan-Apochromat/NA 0.8 objective. Fluorophore excitation and scanning were performed with diode lasers at 405 nm, 488 nm, and 561 nm for Hoechst, Alexa 488, and tdTomato respectively. For cortical length measurements, whole hemispheres were imaged using the Tile-scan mode and a 10× objective, and the superficial surface of layer II/III was measured from the motor cortex to the piriform cortex using ImageJ. For cortical layer markers, the entire cortical thickness corresponding to the region of the somatosensory cortex was imaged using the Tile-scan mode and a 20× objective. Images were analyzed using ImageJ to obtain the whole z stack dataset and measure cortical length.

Statistical Analysis

Mean AAFs of pathogenic somatic mutations identified in FCD and HME cases reported by our study and the published literature were compared using a two-tailed unpaired t test.

SUPPLEMENTAL INFORMATION

Supplemental Information includes Supplemental Experimental Procedures, one figure, and six tables and can be found with this article online at https://doi.org/10.1016/j.celrep.2017.11.106.

ACKNOWLEDGMENTS

We are grateful for the participation of the patients enrolled in our studies. We thank Peter Black, Anne Bergin, Derek Bruce, John Gaitanis, Harvey Sarnat,

Howard Weiner, Mustafa Sahin, Heather Olsen, James Riviello, Farrah Rajabi, Robyn Busch, William Bingaman, Jorge Gonzalez-Martinez, and Katherine Keever for recruiting patients and providing tissue samples and Aldo Rozzo, R. Sean Hill, Jennifer Partlow, and Brenda Barry for logistical assistance. This research was supported in part by the Repository Core for Neurological Disorders, Department of Neurology, Boston Children's Hospital, and the IDDRC (NIH P30HD018655). A.M.D. was supported by the NIGMS (T32GM007753), the NRSA (5T32 GM007226-39), and the Stuart H.Q. & Victoria Quan Fellowship at Harvard Medical School. M.B.W. was supported by the Leonard and Isabelle Goldenson Research Fellowship. A.J.B. was supported by the NINDS (R01NS035129). D.J.K. was supported by the European Commission (602391-2). H.V.V. was supported by the NINDS (NS083823). G.W.M. was supported by the NINDS (R01NS083823 and R01NS038992) and the Davies/Crandall Endowed Chair for Epilepsy Research at UCLA. I.B. was supported by the European Union FP7 Health Program under grant agreement 602531. A.P. was supported by the NINDS (K23NS069784) and the Boston Children's Hospital Translational Research Program. C.A.W. was supported by the NINDS (R01NS079277 and R01 NS035129), the NIMH (U01MH106883), the Allen Discovery Center program through The Paul G. Allen Frontiers Group, and the Manton Center for Orphan Disease Research. C.A.W. is an Investigator of the Howard Hughes Medical Institute.

AUTHOR CONTRIBUTIONS

A.M.D., A.P., and C.A.W. designed the study. C.A.W. supervised the study. A.M.D., M.B.W., A.A.H., S.B., and N.E.H. performed experiments and analyzed data. C.M.L., Z.Y., I.B., D.J.K., H.V.V., J.R.M., and G.W.M. recruited patients and collected and prepared tissue samples. E.Y., Z.Y., I.B., A.J.B., G.W.M., C.A.W., I.N., and A.P. interpreted brain imaging. A.M.D., A.P., and C.A.W. wrote the manuscript, and all coauthors edited the manuscript.

DECLARATION OF INTERESTS

H.V.V. owns stock in several pharmaceutical companies and has received honoraria for lectures (no direct conflict with this paper). G.W.M. serves on the Data Management Committee for Neuropace. I.B. has received honoraria for lectures (no direct conflict with this paper).

Received: June 11, 2017
Revised: October 2, 2017
Accepted: November 29, 2017
Published: December 26, 2017

REFERENCES

Aronica, E., and Crino, P.B. (2014). Epilepsy related to developmental tumors and malformations of cortical development. Neurotherapeutics *11*, 251–268.

Baek, S.T., Copeland, B., Yun, E.J., Kwon, S.K., Guemez-Gamboa, A., Schaffer, A.E., Kim, S., Kang, H.C., Song, S., Mathern, G.W., and Gleeson, J.G. (2015). An AKT3-FOXG1-reelin network underlies defective migration in human focal malformations of cortical development. Nat. Med. *21*, 1445–1454.

Baulac, S., Ishida, S., Marsan, E., Miquel, C., Biraben, A., Nguyen, D.K., Nordli, D., Cossette, P., Nguyen, S., Lambrecq, V., et al. (2015). Familial focal epilepsy with focal cortical dysplasia due to DEPDC5 mutations. Ann. Neurol. *77*, 675–683.

Blümcke, I., and Sarnat, H.B. (2016). Somatic mutations rather than viral infection classify focal cortical dysplasia type II as mTORopathy. Curr. Opin. Neurol. *29*, 388–395.

Blümcke, I., Thom, M., Aronica, E., Armstrong, D.D., Vinters, H.V., Palmini, A., Jacques, T.S., Avanzini, G., Barkovich, A.J., Battaglia, G., et al. (2011). The clinicopathologic spectrum of focal cortical dysplasias: a consensus classification proposed by an ad hoc Task Force of the ILAE Diagnostic Methods Commission. Epilepsia *52*, 158–174.

Blümcke, I., Spreafico, R., Haaker, G., Coras, R., Kobow, K., Bien, C.G., Pfäfflin, M., Elger, C., Widman, G., Schramm, J., et al.; EEBB Consortium (2017). Histopathological Findings in Brain Tissue Obtained during Epilepsy Surgery. N. Engl. J. Med. *377*, 1648–1656.

Cepeda, C., André, V.M., Levine, M.S., Salamon, N., Miyata, H., Vinters, H.V., and Mathern, G.W. (2006). Epileptogenesis in pediatric cortical dysplasia: the dysmature cerebral developmental hypothesis. Epilepsy Behav. *9*, 219–235.

Crino, P.B., Aronica, E., Baltuch, G., and Nathanson, K.L. (2010). Biallelic TSC gene inactivation in tuberous sclerosis complex. Neurology *74*, 1716–1723.

D'Gama, A.M., Geng, Y., Couto, J.A., Martin, B., Boyle, E.A., LaCoursiere, C.M., Hossain, A., Hatem, N.E., Barry, B., Kwiatkowski, D.J., et al. (2015). mTOR pathway mutations cause hemimegalencephaly and focal cortical dysplasia. Ann. Neurol. *77*, 720–725.

Dabora, S.L., Jozwiak, S., Franz, D.N., Roberts, P.S., Nieto, A., Chung, J., Choy, Y.S., Reeve, M.P., Thiele, E., Egelhoff, J.C., et al. (2001). Mutational analysis in a cohort of 224 tuberous sclerosis patients indicates increased severity of TSC2, compared with TSC1, disease in multiple organs. Am. J. Hum. Genet. *68*, 64–80.

Evrony, G.D., Cai, X., Lee, E., Hills, L.B., Elhosary, P.C., Lehmann, H.S., Parker, J.J., Atabay, K.D., Gilmore, E.C., Poduri, A., et al. (2012). Single-neuron sequencing analysis of L1 retrotransposition and somatic mutation in the human brain. Cell *151*, 483–496.

Evrony, G.D., Lee, E., Mehta, B.K., Benjamini, Y., Johnson, R.M., Cai, X., Yang, L., Haseley, P., Lehmann, H.S., Park, P.J., and Walsh, C.A. (2015). Cell lineage analysis in human brain using endogenous retroelements. Neuron *85*, 49–59.

Fu, C., Cawthon, B., Clinkscales, W., Bruce, A., Winzenburger, P., and Ess, K.C. (2012). GABAergic interneuron development and function is modulated by the Tsc1 gene. Cereb. Cortex *22*, 2111–2119.

Gao, P., Postiglione, M.P., Krieger, T.G., Hernandez, L., Wang, C., Han, Z., Streicher, C., Papusheva, E., Insolera, R., Chugh, K., et al. (2014). Deterministic progenitor behavior and unitary production of neurons in the neocortex. Cell *159*, 775–788.

Gorski, J.A., Talley, T., Qiu, M., Puelles, L., Rubenstein, J.L., and Jones, K.R. (2002). Cortical excitatory neurons and glia, but not GABAergic neurons, are produced in the Emx1-expressing lineage. J. Neurosci. *22*, 6309–6314.

Grabiner, B.C., Nardi, V., Birsoy, K., Possemato, R., Shen, K., Sinha, S., Jordan, A., Beck, A.H., and Sabatini, D.M. (2014). A diverse array of cancer-associated MTOR mutations are hyperactivating and can predict rapamycin sensitivity. Cancer Discov. *4*, 554–563.

Harvey, A.S., Cross, J.H., Shinnar, S., and Mathern, G.W.; ILAE Pediatric Epilepsy Surgery Survey Taskforce (2008). Defining the spectrum of international practice in pediatric epilepsy surgery patients. Epilepsia *49*, 146–155.

Hirfanoglu, T., and Gupta, A. (2010). Tuberous sclerosis complex with a single brain lesion on MRI mimicking focal cortical dysplasia. Pediatr. Neurol. *42*, 343–347.

Hoelz, H., Coppenrath, E., Hoertnagel, K., Roser, T., Tacke, M., Gerstl, L., and Borggraefe, I. (2017). Childhood-Onset Epileptic Encephalopathy Associated With Isolated Focal Cortical Dysplasia and a Novel TSC1 Germline Mutation. Clin. EEG Neurosci. Published online March 1, 2017. https://doi.org/10.1177/1550059417697841.

Hoogeveen-Westerveld, M., Wentink, M., van den Heuvel, D., Mozaffari, M., Ekong, R., Povey, S., den Dunnen, J.T., Metcalfe, K., Vallee, S., Krueger, S., et al. (2011). Functional assessment of variants in the TSC1 and TSC2 genes identified in individuals with Tuberous Sclerosis Complex. Hum. Mutat. *32*, 424–435.

Jamuar, S.S., Lam, A.T., Kircher, M., D'Gama, A.M., Wang, J., Barry, B.J., Zhang, X., Hill, R.S., Partlow, J.N., Rozzo, A., et al. (2014). Somatic mutations in cerebral cortical malformations. N. Engl. J. Med. *371*, 733–743.

Jansen, L.A., Mirzaa, G.M., Ishak, G.E., O'Roak, B.J., Hiatt, J.B., Roden, W.H., Gunter, S.A., Christian, S.L., Collins, S., Adams, C., et al. (2015). PI3K/AKT pathway mutations cause a spectrum of brain malformations from megalencephaly to focal cortical dysplasia. Brain *138*, 1613–1628.

Jones, A.C., Shyamsundar, M.M., Thomas, M.W., Maynard, J., Idziaszczyk, S., Tomkins, S., Sampson, J.R., and Cheadle, J.P. (1999). Comprehensive

mutation analysis of TSC1 and TSC2-and phenotypic correlations in 150 families with tuberous sclerosis. Am. J. Hum. Genet. *64*, 1305–1315.

Kingsmore, S., Smith, L., Soden, S., Dinwiddie, D., Saunders, C., Farrow, E., Miller, N., Abdelmoity, A., and Atherton, A. (2013). Exome Sequencing Reveals De Novo Germline Mutation of the Mammalian Target of Rapamycin (MTOR) in a Patient with Megalencephaly and Intractable Seizures. Journal of Genomes and Exomes *2*, 63–72.

Knudson, A.G., Jr. (1971). Mutation and cancer: statistical study of retinoblastoma. Proc. Natl. Acad. Sci. USA *68*, 820–823.

Kurek, K.C., Luks, V.L., Ayturk, U.M., Alomari, A.I., Fishman, S.J., Spencer, S.A., Mulliken, J.B., Bowen, M.E., Yamamoto, G.L., Kozakewich, H.P., and Warman, M.L. (2012). Somatic mosaic activating mutations in PIK3CA cause CLOVES syndrome. Am. J. Hum. Genet. *90*, 1108–1115.

Kwan, P., Arzimanoglou, A., Berg, A.T., Brodie, M.J., Allen Hauser, W., Mathern, G., Moshé, S.L., Perucca, E., Wiebe, S., and French, J. (2010). Definition of drug resistant epilepsy: consensus proposal by the ad hoc Task Force of the ILAE Commission on Therapeutic Strategies. Epilepsia *51*, 1069–1077.

Lal, D., Reinthaler, E.M., Schubert, J., Muhle, H., Riesch, E., Kluger, G., Jabbari, K., Kawalia, A., Bäumel, C., Holthausen, H., et al. (2014). DEPDC5 mutations in genetic focal epilepsies of childhood. Ann. Neurol. *75*, 788–792.

Lee, J.H., Huynh, M., Silhavy, J.L., Kim, S., Dixon-Salazar, T., Heiberg, A., Scott, E., Bafna, V., Hill, K.J., Collazo, A., et al. (2012). De novo somatic mutations in components of the PI3K-AKT3-mTOR pathway cause hemimegalencephaly. Nat. Genet. *44*, 941–945.

Lim, J.S., Kim, W.I., Kang, H.C., Kim, S.H., Park, A.H., Park, E.K., Cho, Y.W., Kim, S., Kim, H.M., Kim, J.A., et al. (2015). Brain somatic mutations in MTOR cause focal cortical dysplasia type II leading to intractable epilepsy. Nat. Med. *21*, 395–400.

Lim, J.S., Gopalappa, R., Kim, S.H., Ramakrishna, S., Lee, M., Kim, W.I., Kim, J., Park, S.M., Lee, J., Oh, J.H., et al. (2017). Somatic Mutations in TSC1 and TSC2 Cause Focal Cortical Dysplasia. Am. J. Hum. Genet. *100*, 454–472.

Lindhurst, M.J., Sapp, J.C., Teer, J.K., Johnston, J.J., Finn, E.M., Peters, K., Turner, J., Cannons, J.L., Bick, D., Blakemore, L., et al. (2011). A mosaic activating mutation in AKT1 associated with the Proteus syndrome. N. Engl. J. Med. *365*, 611–619.

Lipton, J.O., and Sahin, M. (2014). The neurology of mTOR. Neuron *84*, 275–291.

Lodato, M.A., Woodworth, M.B., Lee, S., Evrony, G.D., Mehta, B.K., Karger, A., Lee, S., Chittenden, T.W., D'Gama, A.M., Cai, X., et al. (2015). Somatic mutation in single human neurons tracks developmental and transcriptional history. Science *350*, 94–98.

Magri, L., Cominelli, M., Cambiaghi, M., Cursi, M., Leocani, L., Minicucci, F., Poliani, P.L., and Galli, R. (2013). Timing of mTOR activation affects tuberous sclerosis complex neuropathology in mouse models. Dis. Model. Mech. *6*, 1185–1197.

Meikle, L., Talos, D.M., Onda, H., Pollizzi, K., Rotenberg, A., Sahin, M., Jensen, F.E., and Kwiatkowski, D.J. (2007). A mouse model of tuberous sclerosis: neuronal loss of Tsc1 causes dysplastic and ectopic neurons, reduced myelination, seizure activity, and limited survival. J. Neurosci. *27*, 5546–5558.

Mirzaa, G.M., Conti, V., Timms, A.E., Smyser, C.D., Ahmed, S., Carter, M., Barnett, S., Hufnagel, R.B., Goldstein, A., Narumi-Kishimoto, Y., et al. (2015). Characterisation of mutations of the phosphoinositide-3-kinase regulatory subunit, PIK3R2, in perisylvian polymicrogyria: a next-generation sequencing study. Lancet Neurol. *14*, 1182–1195.

Mirzaa, G.M., Campbell, C.D., Solovieff, N., Goold, C., Jansen, L.A., Menon, S., Timms, A.E., Conti, V., Biag, J.D., Adams, C., et al. (2016). Association of MTOR Mutations With Developmental Brain Disorders, Including Megalencephaly, Focal Cortical Dysplasia, and Pigmentary Mosaicism. JAMA Neurol. *73*, 836–845.

Møller, R.S., Weckhuysen, S., Chipaux, M., Marsan, E., Taly, V., Bebin, E.M., Hiatt, S.M., Prokop, J.W., Bowling, K.M., Mei, D., et al. (2016). Germline and somatic mutations in the MTOR gene in focal cortical dysplasia and epilepsy. Neurol. Genet. *2*, e118.

Nakashima, M., Saitsu, H., Takei, N., Tohyama, J., Kato, M., Kitaura, H., Shiina, M., Shirozu, H., Masuda, H., Watanabe, K., et al. (2015). Somatic Mutations in the MTOR Gene Cause Focal Cortical Dysplasia Type IIb. Ann. Neurol. *78*, 375–386.

Poduri, A. (2014). DEPDC5 does it all: shared genetics for diverse epilepsy syndromes. Ann. Neurol. *75*, 631–633.

Poduri, A., Evrony, G.D., Cai, X., Elhosary, P.C., Beroukhim, R., Lehtinen, M.K., Hills, L.B., Heinzen, E.L., Hill, A., Hill, R.S., et al. (2012). Somatic activation of AKT3 causes hemispheric developmental brain malformations. Neuron *74*, 41–48.

Qin, W., Chan, J.A., Vinters, H.V., Mathern, G.W., Franz, D.N., Taillon, B.E., Bouffard, P., and Kwiatkowski, D.J. (2010). Analysis of TSC cortical tubers by deep sequencing of TSC1, TSC2 and KRAS demonstrates that small second-hit mutations in these genes are rare events. Brain Pathol. *20*, 1096–1105.

Roy, A., Skibo, J., Kalume, F., Ni, J., Rankin, S., Lu, Y., Dobyns, W.B., Mills, G.B., Zhao, J.J., Baker, S.J., and Millen, K.J. (2015). Mouse models of human PIK3CA-related brain overgrowth have acutely treatable epilepsy. eLife *4*, e12703.

Scheffer, I.E., Heron, S.E., Regan, B.M., Mandelstam, S., Crompton, D.E., Hodgson, B.L., Licchetta, L., Provini, F., Bisulli, F., Vadlamudi, L., et al. (2014). Mutations in mammalian target of rapamycin regulator DEPDC5 cause focal epilepsy with brain malformations. Ann. Neurol. *75*, 782–787.

Sim, J.C., Scerri, T., Fanjul-Fernández, M., Riseley, J.R., Gillies, G., Pope, K., van Roozendaal, H., Heng, J.I., Mandelstam, S.A., McGillivray, G., et al. (2016). Familial cortical dysplasia caused by mutation in the mammalian target of rapamycin regulator NPRL3. Ann. Neurol. *79*, 132–137.

Tyburczy, M.E., Dies, K.A., Glass, J., Camposano, S., Chekaluk, Y., Thorner, A.R., Lin, L., Krueger, D., Franz, D.N., Thiele, E.A., et al. (2015a). Mosaic and Intronic Mutations in TSC1/TSC2 Explain the Majority of TSC Patients with No Mutation Identified by Conventional Testing. PLoS Genet. *11*, e1005637.

Tyburczy, M.E., Jozwiak, S., Malinowska, I.A., Chekaluk, Y., Pugh, T.J., Wu, C.L., Nussbaum, R.L., Seepo, S., Dzik, T., Kotulska, K., and Kwiatkowski, D.J. (2015b). A shower of second hit events as the cause of multifocal renal cell carcinoma in tuberous sclerosis complex. Hum. Mol. Genet. *24*, 1836–1842.

Uhlmann, E.J., Wong, M., Baldwin, R.L., Bajenaru, M.L., Onda, H., Kwiatkowski, D.J., Yamada, K., and Gutmann, D.H. (2002). Astrocyte-specific TSC1 conditional knockout mice exhibit abnormal neuronal organization and seizures. Ann. Neurol. *52*, 285–296.

Weckhuysen, S., Marsan, E., Lambrecq, V., Marchal, C., Morin-Brureau, M., An-Gourfinkel, I., Baulac, M., Fohlen, M., Kallay Zetchi, C., Seeck, M., et al. (2016). Involvement of GATOR complex genes in familial focal epilepsies and focal cortical dysplasia. Epilepsia *57*, 994–1003.

Xue, Y., and Wilcox, W.R. (2016). Changing paradigm of cancer therapy: precision medicine by next-generation sequencing. Cancer Biol. Med. *13*, 12–18.

Zeng, L.H., Rensing, N.R., Zhang, B., Gutmann, D.H., Gambello, M.J., and Wong, M. (2011). Tsc2 gene inactivation causes a more severe epilepsy phenotype than Tsc1 inactivation in a mouse model of tuberous sclerosis complex. Hum. Mol. Genet. *20*, 445–454.

Zhou, J., Blundell, J., Ogawa, S., Kwon, C.H., Zhang, W., Sinton, C., Powell, C.M., and Parada, L.F. (2009). Pharmacological inhibition of mTORC1 suppresses anatomical, cellular, and behavioral abnormalities in neural-specific Pten knock-out mice. J. Neurosci. *29*, 1773–1783.